

wavelength scale greater than the entanglement separation. The slow relaxation manifests itself at a concentration which appears to be related to the chain geometry. Thus, slow relaxations are observed in the PEO/H₂O system at a concentration lower by an order of magnitude than that for polystyrene in benzene.¹² There is good evidence³⁰ for binding of water molecules to the PEO chain in the ratio 2:1. Such hydrogen-bonding interactions with the chain are undoubtedly a factor determining the relatively high chain extension. PEO has, for example, a much greater intrinsic viscosity than polystyrene in good solvents; furthermore, the ratio (R_G^2/M) is reported³² to be 10 times larger than for polystyrene in toluene. However, the relationships between concentration, chain extension, polymer-solvent interaction and geometric entanglement still require elucidation. The present measurements only provide support for the view that these quantities are of central importance. It is noted that a model for the coupling between internal modes and anisotropic translational diffusion in congested solutions has been put forward by Lee et al.,³⁵ who describe dynamic light scattering measurements on DNA.

Registry No. Poly(ethylene oxide), 25322-68-3; polystyrene, 9003-53-6.

References and Notes

- (1) Nose, T.; Chu, B. *Macromolecules* **1979**, *12*, 590.
- (2) Chu, B.; Nose, T. *Macromolecules* **1980**, *13*, 122.
- (3) Mathiez, P.; Mouttet, C.; Weisbuch, G. *J. Phys. (Paris)* **1980**, *41*, 519. See also: *Biopolymers* **1979**, *18*, 1465; **1981**, *20*, 2381.
- (4) Nishio, I.; Wada, A. *Polym. J.* **1980**, *12*, 145.
- (5) Reihanian, H.; Jamieson, A. M. *Macromolecules* **1979**, *12*, 684.
- (6) Yu, T. L.; Reihanian, H.; Jamieson, A. M. *Macromolecules* **1980**, *13*, 1590.
- (7) Southwick, J. G.; Jamieson, A. M.; Blackwell, J. *Macromolecules* **1981**, *14*, 1728.
- (8) Amis, E. J.; Janmey, P. A.; Ferry, J. D.; Yu, H. *Polym. Bull.* **1981**, *6*, 13.
- (9) Amis, E. J.; Han, C. C. *Polymer* **1982**, *23*, 1403.
- (10) Nyström, B.; Roots, J. *Prog. Polym. Sci.* **1982**, *8*, 333.
- (11) Brown, W.; Johnsen, R. M.; Stilbs, P. *Polym. Bull.* **1983**, *9*, 305.
- (12) Brown, W., *Polymer*, in press.
- (13) de Gennes, P.-G. *Macromolecules* **1976**, *9*, 587, 594. Also in: "Scaling Concepts in Polymer Physics"; Cornell University Press, Ithaca, NY, 1979.
- (14) Brown, W.; Johnsen, R. M.; Stilbs, P. *J. Polym. Sci., Polym. Phys. Ed.* **1983**, *21*, 1029.
- (15) Roots, J.; Nyström, B. *Macromolecules* **1981**, *14*, 1728.
- (16) Koppel, D. E. *J. Chem. Phys.* **1972**, *57*, 4814.
- (17) Patterson, G. D.; Jarry, J.-P.; Lindsey, C. P. *Macromolecules* **1980**, *13*, 668.
- (18) Callaghan, P. T.; Pinder, D. N. *Macromolecules* **1981**, *14*, 1334.
- (19) Léger, L.; Hervet, H.; Rondelez, F. *Macromolecules* **1981**, *14*, 1732.
- (20) Brown, W.; Stilbs, P.; Johnsen, R. M. *J. Polym. Sci., Polym. Phys. Ed.* **1982**, *20*, 1771.
- (21) Simha, R.; Zakin, J. L. *J. Chem. Phys.* **1960**, *33*, 1791.
- (22) Klein, J. *Macromolecules* **1978**, *11*, 852.
- (23) Ferry, J. D. In "Viscoelastic Properties of Polymers", 3rd ed.; Wiley: New York, 1980.
- (24) Polik, W. F.; Burchard, W. *Macromolecules* **1983**, *16*, 978.
- (25) Roots, J.; Nyström, B.; Porsch, B.; Sundelöf, J.-O. *Polymer* **1979**, *20*, 337.
- (26) Bailey, D.; King, T. A.; Pinder, D. W. *Chem. Phys.* **1976**, *12*, 161.
- (27) Allen, G.; Vasudevan, P.; Hawkins, E. Y.; King, T. A. *J. Chem. Soc., Faraday Trans. 2* **1977**, *73*, 449.
- (28) Munch, J.-P.; Hild, G.; Candau, S.; *Macromolecules* **1983**, *16*, 71.
- (29) Brochard, F.; de Gennes, P.-G. *Macromolecules* **1977**, *10*, 1157.
- (30) Molyneux, P. In "Water, A Comprehensive Treatise"; Franks, F., Ed.; Plenum Press: New York, 1975; Vol. 4, p 569.
- (31) Cornet, C. F. *Polymer* **1965**, *6*, 373.
- (32) Kambe, Y.; Chikato, H. *Rep. Prog. Polym. Phys.* **1982**, *25*, 121.
- (33) Koene, R. S.; Mandel, M. *Macromolecules* **1983**, *16*, 220, 978.
- (34) Koene, R. S.; Nicolai, T.; Mandel, M. *Macromolecules* **1983**, *16*, 227, 231.
- (35) Lee, W. I.; Schmitz, K. S.; Lin, S.-C.; Schurr, J. M. *Biopolymers* **1977**, *16*, 583.

ESR Investigation of Molecular Motion in Thermotropic Liquid Crystalline Polyesters Containing Nitroxide Spin Probes

Patrick Meurisse,[†] Claude Friedrich,[†] Maya Dvolaitzky,[†]
Françoise Lauprêtre,[†] Claudine Noël,^{*,†} and Lucien Monnerie[†]

Laboratoire de Physicochimie Structurale et Macromoléculaire, ESPCI,
75231 Paris Cedex 05, France, and Laboratoire de Physique de la Matière Condensée,
Collège de France, 75231 Paris Cedex 05, France. Received July 15, 1982

ABSTRACT: Two aromatic-aliphatic polyesters $\text{-CO(p-C}_6\text{H}_4)_3\text{COO(CH}_2\text{CH}_2\text{O)}_n\text{-}$, abbreviated TO11 and TO29 for $n = 4$ and $n = 10$, respectively, which form liquid crystalline phases, were investigated. The ESR spectra of these polyesters doped with various nitroxide radicals were recorded at 108–413 K and were given a preliminary interpretation with a model of isotropic rotational reorientation. Such an analysis argues for a glass transition temperature T_{gl} at 223–263 K with a second T_{gv} at 293–333 K. A more careful analysis of the spectra by using a model of anisotropic rotational reorientation showed that below the crystal \leftrightarrow mesophase transition (i.e., the melting point) the axis z' of the rotational diffusion tensor describing this rotational reorientation was an axis perpendicular to that of the N–O bond and that, depending on the length of the "ether" sequence, the rotational reorientation about this axis is 2–7 times faster than about the remaining two axes. The observed changes in the ESR spectra of probes as they pass through the crystal \leftrightarrow mesophase transition are explained in terms of a change in the anisotropic rotation of probes.

Introduction

There is now a considerable body of literature dealing with thermotropic liquid crystalline polymers that melt to give fluid anisotropic phases whose textures and prop-

erties appear similar to those observed with low molecular weight liquid crystals. So far, most of the work has focused on the search for newer and newer polymers and the study of their structures as liquid crystalline phases.¹ By contrast, only a few attempts have been made to give a detailed explanation of the relaxation processes in these materials.^{2–5} Since the detection and evaluation of polymer motions may aid in correlating polymer structure with observed mechanical properties, it seems of interest to

[†]Laboratoire de Physicochimie Structurale et Macromoléculaire, ESPCI.

^{*}Laboratoire de Physique de la Matière Condensée, Collège de France.

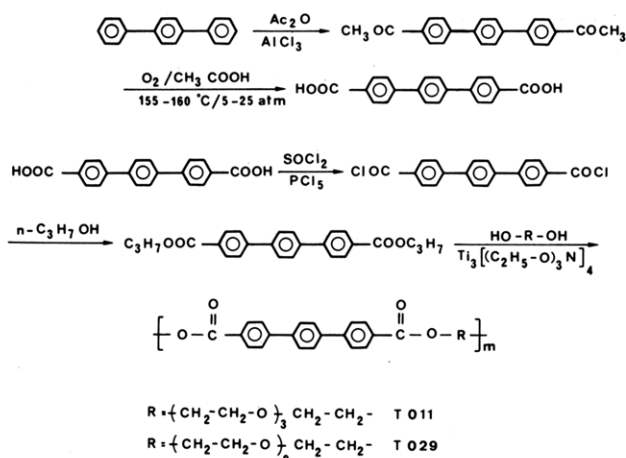
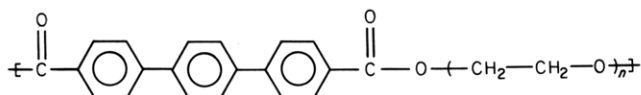


Figure 1. Synthetic route for the preparation of polyesters TO29 and TO11.

investigate the dynamics of such polymers on a molecular level.

The ESR spin-probe technique has proved to be a powerful tool for investigating the translational and reorientational motions of whole molecules or parts of molecules. An investigation of the ESR spectra of stable nitroxide radicals added to the polymer matrix allows one to obtain information on the way in which the rotational reorientation of the probe, characterized by a temperature-dependent correlation time, is affected by the polymer motions.⁶ Defining the exact relationship between observed relaxation times and internal motions of a polymer can be quite complex, however. One way to increase the overall amount of relaxation information is to work with polymers whose structures are slightly different. To start such an investigation we used the two thermotropic liquid crystalline polyesters



abbreviated TO11 and TO29 for $n = 4$ and $n = 10$, respectively. The interesting feature of these two semi-crystalline polymers is that they exhibit several transitions when cooled from the isotropic liquid state.¹⁸ Taking into account all the data of the different ESR spin-probe experiments and comparing experimental spectra to those calculated under certain assumptions, we want to derive some conclusions concerning the dynamics of these phases. Some of our results were presented at the 10th Europhysics Conference on Macromolecular Physics: "Structure and Motion in Polymeric Glasses", Noordwijkerhout (21-25 Apr 1980)

Experimental Section

Materials. The polyesters TO11 and TO29 were prepared at the Centre de Recherches des Carrières de Rhone-Poulenc (Saint-Fons, France) by standard methods via the scheme given in Figure 1.¹⁸ Details of the polyesters' properties are given in ref 1g, 2, 7, and 8. To summarize: at room temperature, TO11 and TO29 have inherent viscosities of 0.6 and 0.69 dL/g at a polymer concentration of 0.6 g/dL in dichloroacetic acid. DSC curves (Figure 2) show two marked endotherms. For polyester TO11, the highest temperature peak ($\sim 250^\circ\text{C}$) corresponds to a transition from a liquid crystalline to an isotropic phase. Changes in the X-ray diffraction patterns of TO11, commencing at 125°C , were interpreted as a transition from the solid to a S_c phase. Such a mesophase is usually described as a layered system made by the superposition of two-dimensional liquid layers. In these layers the molecules are tilted with respect to the normal to the layers. Besides, it can be seen from X-ray investigation⁷

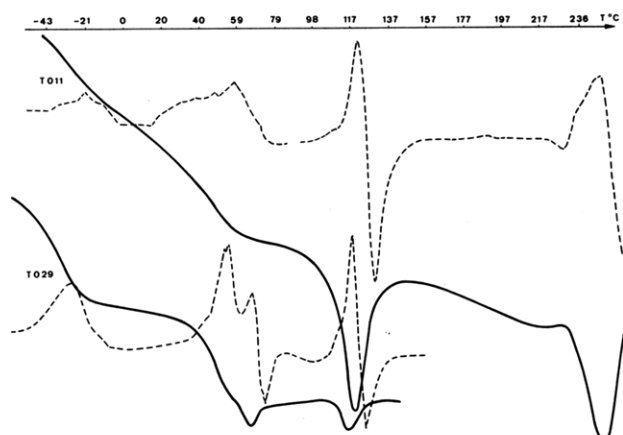


Figure 2. DSC curves of polyesters TO29 and TO11. Samples were purified by dissolution in chloroform and precipitation in methanol before being dried under vacuum at room temperature. The dashed lines are derivative curves.

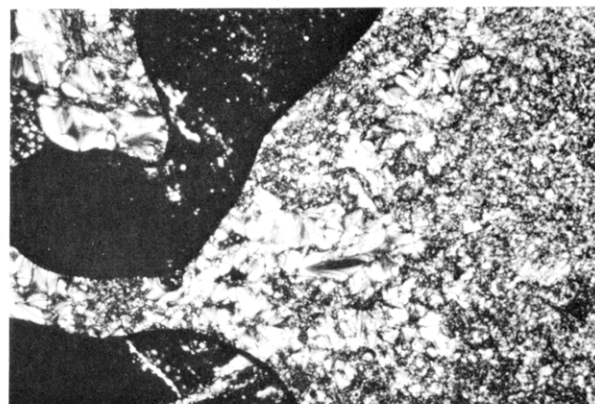


Figure 3. Photomicrograph of smectic C mesophase from polyester TO11 at 240°C . Focal conic texture (crossed polarizers).

that the relatively short flexible spacers adopt a single, entirely extended trans conformation. Such a behavior helps in establishing equal-length flexible spacers and favors the parallel alignment of rigid core parts of the molecules. Phenylene rings play more than a purely geometrical role in stabilizing such an ordered arrangement of the molecules. It seems that the π -electron system of aromatic rings, being polarizable and permitting conjugative interactions, must give rise to suitably strong intermolecular attractions that are anisotropic and stabilize the S_c phase of molecules with the centers of mass of the segments segregated into layers. The assignment of the S_c phase was confirmed by polarized-light photomicrographs depicting the appearance of the TO11 mesophase in the temperature range $125\text{--}250^\circ\text{C}$. As illustrated in Figure 3 they exhibit characteristic features of S_c phases. Miscibility studies were also consistent with the formation of a S_c phase. Indeed, the TO11 mesophase was found to be miscible with the S_c phase of the standard material terephthalidenebis(4-*n*-butylaniline).⁸ By contrast, above the melting point ($\sim 70^\circ\text{C}$), polyester TO29 shows distinct phases of liquid crystal and isotropic liquid (Figure 4). The mesophase is characterized by a diffuse halo around $q = 4\pi(\sin \theta)/\lambda \simeq 1.4 \text{ \AA}^{-1}$, which is consistent with a nematic structure (the mean feature of molecular organization is the orientational order of the molecular long axes; the periodicity of molecular arrangement in the smectic phase is absent in the nematic phase, and the centers of the rigid mesogenic groups are distributed at random as in the amorphous liquid). It should be pointed out now that long flexible spacers are not usually favorable to liquid crystal formation. This reflects the decreasing thermal stability of the mesophase with decreasing polarity (dilution of the effective number of aromatic mesogenic groups) and molecular rigidity. Indeed, such long segments are capable of adopting more or less coiled conformations and favor a nonparallel arrangement of the molecules. Thus, the coexistence of a "nematic" phase and an isotropic phase in polyester TO29 is probably due to the polydispersity of the low molecular weight

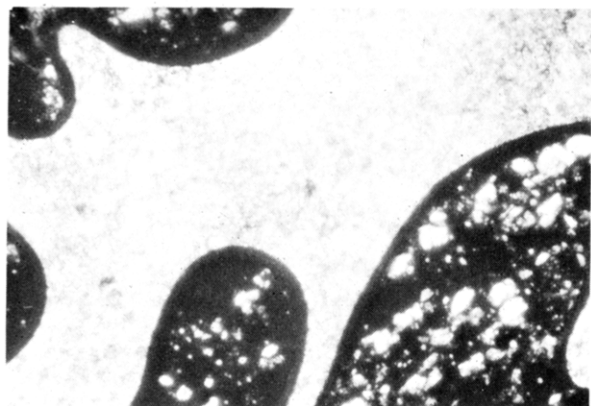


Figure 4. Liquid crystalline and isotropic phases of polyester TO29 at 90 °C.

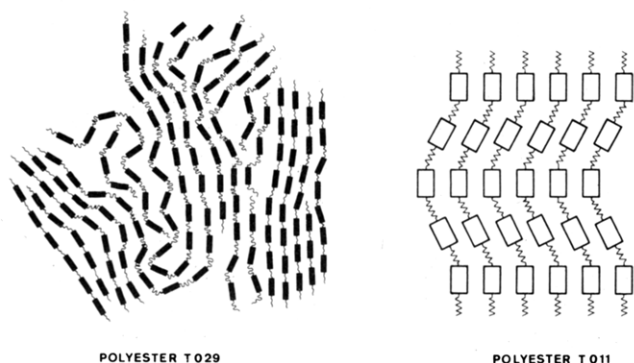


Figure 5. Distribution of macromolecular chains in polyesters TO29 and TO11.

(H400) fraction of PEO used for preparing polyester TO29. Optical observations and X-ray diffraction patterns reveal that in the temperature range 117–125 °C, the liquid crystalline phase disappears. Polyester TO29 becomes completely isotropic.

In Figure 5 we schematically illustrate how polyesters TO11 and TO29 can adopt organizations compatible with the results obtained below 250 and 117–125 °C, respectively. This would be consistent for polyester TO29 with the formation at low temperatures of an amorphous isotropic glass and an anisotropic glass with the long-range order of "nematic" liquid crystals. Hence, it seems reasonable to associate the increases in heat capacity observed between –50 and –10 °C and 20–60 °C (Figure 2) with the glass transitions of the isolated disordered structure (T_{gi}) and the ordered material under restraint by crystallites (T_{gu}), respectively. T_{gu} is not a definite, fixed value. It can be seen from Figure 6 that on annealing, T_{gi} appears always in the same temperature range, while T_{gu} slightly shifts to higher temperature. By contrast, because of the much higher content of ordered structure, one expects only one glass transition for polyester TO11. Thus, it seems reasonable to associate the marked increase in heat capacity evidenced between 20 and 60 °C (Figure 2) with the locking in of the smectic phase organization through cooling. Only the samples that have been rapidly quenched from the isotropic state (i.e., $T > 250$ °C) exhibit a marked increase in heat capacity in the T_{gi} temperature range. From the temperature dependence of the proton-decoupled ^{13}C solid-state NMR line shapes, Sergot et al.² have shown that the motion of some methylene carbons is already obvious at room temperature while the spectra of the aromatic carbons are those of the rigid lattice until the melting point.

ESR Measurements. The spin probes chosen for this work were 2,2,6,6-tetramethyl-4-hydroxypiperidinyl-1-oxy (A), two derivatives of 2,2,5,5-tetramethylpyrrolidine 1-oxide (B and C), and one oxazolidine derivative (D) (Figure 7). The nitroxide spin probes A and D were prepared by standard methods.^{9–11} Probe radicals B and C were obtained from Eastman Kodak.

A speck of nitroxide radical was mixed with the polyester, taking care that the concentration of spin probe did not exceed 0.01% by weight. The mixture was packed in ESR tubes, heated to the

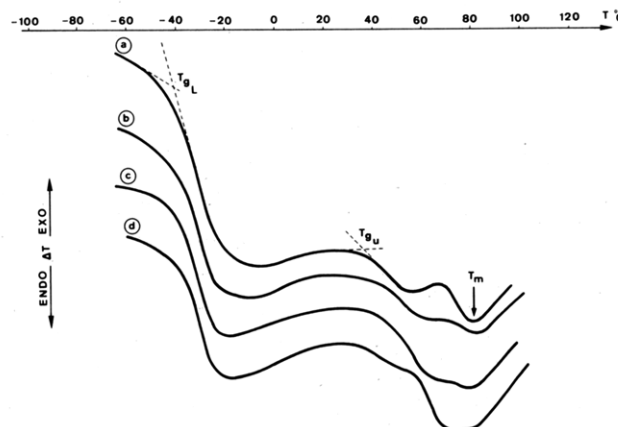


Figure 6. Effect of the annealing temperature on T_{gL} and T_{gu} for polyester TO29. With the exception of the unannealed sample (a), the samples used were annealed for 1 h at 40 °C (b), 45 °C (c), and 50 °C (d).

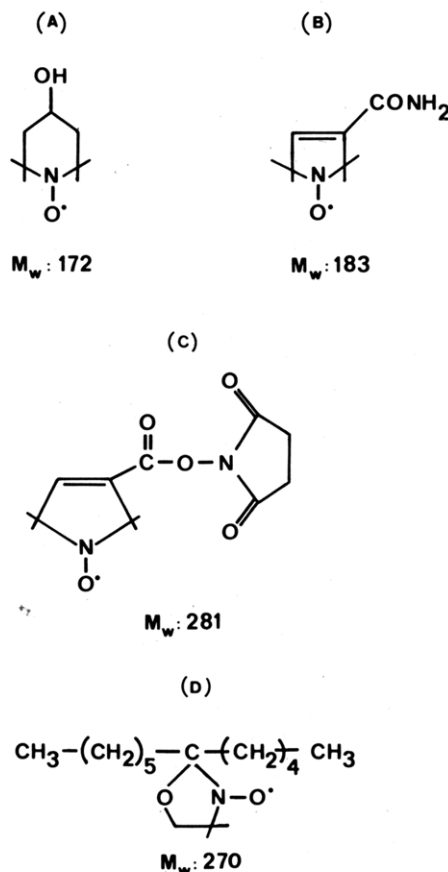


Figure 7. Structure and molecular weight of nitroxide spin probes.

corresponding isotropic temperature, and stirred continuously until the spin probe was homogeneously mixed with the polyester. Samples were sealed off under dynamic vacuum in ESR tubes after repeated freeze-pump-thaw cycles.

ESR spectra were recorded with a Varian E-4 X-band spectrometer. The temperature of the samples was controlled with a Varian E-257 variable-temperature accessory and measured by a copper-constantan thermocouple lowered into the cavity before and after each series of measurements.

In the case of low molecular weight compounds, aligned nematics or smectics can be obtained only by cooling the sample from the isotropic to the nematic or smectic phase in the presence of a strong magnetic field (~ 10 kG).¹² Such a field is sufficient to impose the character of a single crystal on the mesophase. The molecules are oriented such that only thermal vibrations occur and they are directed along one principal axis as determined by

the direction of the field. Such aligned samples are required for determining the orientational order parameter \overline{P}_2 . In contrast to conventional liquid crystals, only a few polymers containing mesogenic moieties and flexible spacers in the main chain orient in a magnetic field.¹³⁻¹⁶ The ease of orientation seems to depend on the chemical structure: the shorter the length of the flexible spacer, the easier the orientation.¹⁷ We did not succeed in obtaining macroscopically aligned polyesters either by applying a strong magnetic field (~ 10 kG) or by using glass surface treatments. Both in the solid and liquid crystalline state the ESR spectra did not reveal any angular dependence, which is characteristic of polycrystalline and mesomorphic polydomain samples.

Theory

The dominant electron spin relaxation processes of a nitroxide radical diluted in a diamagnetic host are the motional modulation of the anisotropic electron Zeeman g and electron nuclear hyperfine A interactions. A general solution of the ESR line shape problem covering both the fast- and slow-tumbling regions has been presented by Freed and co-workers.^{18,19} It is based on the stochastic Liouville equation and assumes a Markoffian stochastic modulation of $\mathcal{H}_1(t)$, the rotational-dependent perturbation in the spin Hamiltonian. A number of different models for rotational reorientation of the spin probe can be proposed. Some useful ones are Brownian rotational diffusion, simplified models of free diffusion, and diffusion by jumps of substantial angle. A computer program for line shape simulation is given in Appendix B, Chapter 3, of ref 19.

The line shape theory developed by Freed is the most accurate method for analyzing ESR spectra in terms of spin-probe motion. However, under certain conditions, simplifying assumptions can be made. In this regard, it is of interest to distinguish the fast-motional region corresponding to correlation times τ_c in the range 5×10^{-11} to 10^{-9} s and the slow-tumbling one (10^{-9} s $< \tau_c < 10^{-7}$ s).

(a) Fast-Motional Region. In the case of rapid reorientations, the spectrum of a nitroxide spin probe has been shown to consist of three Lorentzian lines, corresponding to each value ($M = +1, 0, -1$) of the ^{14}N nuclear projection quantum number.

In general, the dependence of the spectral line width upon M , the component of the nuclear spin along the direction of the applied magnetic field, is given by

$$T_2^{-1}(M) = A + BM + CM^2 + \chi$$

where χ is the intrinsic line width, which takes into account other contributions to $T_2^{-1}(M)$ such as the spin-rotational interactions, the unresolved proton hyperfine splitting, and instrumental broadening. Reference should be made to the original literature^{20,21} and excellent reviews^{22,23} for details of this analysis.

For the case of *anisotropic* rotational diffusion, that is to say assuming that the spin-probe reorientation can be described by the diffusion equation of an axially symmetric ellipsoid with coefficients D_{\parallel} and D_{\perp} coincident with the \mathbf{g} and \mathbf{A} magnetic tensor axes and neglecting the non-spherical Hamiltonian terms, A , B , and C are written as

$$A = \frac{2}{15} \frac{\omega_0^2}{g^2} \{ (F_g^0)^2 \tau_0 + 2(F_g^2)^2 \tau_2 \} + \frac{I(I+1)}{20} \{ (F_A^0)^2 \tau_0 + 2(F_A^2)^2 \tau_2 \} \quad (1a)$$

$$B = \frac{4}{15} \frac{\omega_0}{g} \{ F_g^0 F_A^0 \tau_0 + 2F_g^2 F_A^2 \tau_2 \} \quad (1b)$$

$$C = \frac{1}{12} \{ (F_A^0)^2 \tau_0 + 2(F_A^2)^2 \tau_2 \} \quad (1c)$$

with

$$F_A^0 = (2/3)^{1/2} [A_z - 1/2(A_x + A_y)]$$

$$F_g^0 = (2/3)^{1/2} [g_z - 1/2(g_x + g_y)]$$

$$F_A^2 = 1/2(A_x - A_y)$$

$$F_g^2 = 1/2(g_x - g_y)$$

$F_A^0, F_A^2, F_g^0, F_g^2$ are the irreducible components of the nitrogen hyperfine and \mathbf{g} tensors calculated in the principal coordinate system of the diffusion tensor,²³ I is the nitrogen nuclear spin quantum number, and ω_0 is the frequency of the microwave transitions. The two correlation times τ_0 and τ_2 are defined by

$$\tau_0^{-1} = 6D_{\perp} \quad \tau_2^{-1} = 2D_{\perp} + 4D_{\parallel}$$

They are assumed to obey the following inequalities:

$$\omega_0^2 \tau_0^2 \gg 1 \quad \omega_0^2 \tau_2^2 \gg 1$$

$$\omega_{\text{hf}}^2 \tau_0^2 \ll 1 \quad \omega_{\text{hf}}^2 \tau_2^2 \ll 1$$

where ω_{hf} is the hyperfine splitting in angular frequency units.

For an *isotropic* rotation of the probe, $\tau_0 = \tau_2 = \tau_c$ (which is defined as $\tau_c = (6\bar{D})^{-1}$, with $\bar{D} = (D_3 D_1)^{1/2}$; D_1 and D_3 are the principal components of the diffusion tensor) and the following relation can be derived:

$$\frac{C}{B} = \frac{15}{48} \frac{g}{\omega_0} \frac{[(F_A^0)^2 + 2(F_A^2)^2]}{F_A^0 F_g^0 + 2F_A^2 F_g^2} = K \quad (2)$$

K is a constant that only depends on the anisotropic components of the hyperfine tensor \mathbf{A} and \mathbf{g} tensor.

With the ratios $T_2(0)/T_2(+1)$ and $T_2(0)/T_2(-1)$ defined as R_+ and R_- it is readily shown that

$$R_+ + R_- - 2 = 2CT_2(0) \quad (3)$$

Making the assumption of axial symmetry in the hyperfine interaction tensor leads to

$$R_+ + R_- - 2 = \frac{b^2}{4} T_2(0) \tau \quad (4)$$

where $b = 2/3(A_{\parallel} - A_{\perp})$ and $T_2^{-1}(0)$ is the width of the central line that corresponds to $M = 0$. Experimental values $T_2(0)/T_2(\pm 1)$ are obtained from the square root of the ratios of the experimental derivative curve peak heights. The magnetic parameters of the spin probes are summarized in Table I.

(b) Slow-Tumbling Region. Computer simulation of experimental spectra is the best method for treating anisotropic rotational reorientation and slow tumbling, but it is sometimes impossible to apply the analysis developed by Freed and co-workers. Indeed, it needs (i) to make a sensible estimate of the direction cosines between the principal axes of the diffusion tensor and those of the hyperfine and \mathbf{g} tensors and (ii) an accurate determination of the anisotropic components of the hyperfine and \mathbf{g} tensors. For this reason, simplified methods for estimating the rotational correlation time τ_c have been developed, based on quantities that can be directly obtained from experimental spectra. In particular, one needs only to measure $S = A_z'/A_z$, where A_z' is half the separation of the outer hyperfine extrema and A_z is the rigid-limit value for the same quantity.²⁶ More precisely, Goldman et al.^{26a} have found that for spherical spin probes

$$\tau_c = a(1 - S)^b \quad (10^{-9} < \tau_c < 10^{-7} \text{ s})$$

Table I
Magnetic Parameters of Spin Probes^a

spin probe	A_0 , G	g_0	A_{\parallel} , G	A_{\perp} , G	g_{\parallel}	g_{\perp}
A ^b	15.66	2.0055	35.8	5.6	2.0022	2.0072
B	14.6	2.0061	33.8	5	2.0032	2.0076
C	14.38	2.0058	33.62	4.76	2.0032	2.0071
D	14.55	2.0059	34	4.825	2.0027	2.0074

^a Magnetic parameters A_{\parallel} and g_{\parallel} and A_0 and g_0 were determined by an analysis of the spectra measured in *p*-chloronaphthalene at 113 and 393 K, respectively. Combining the value of A_0 with that of A_{\parallel} and making the assumption of axial symmetry in the hyperfine interaction tensor leads to A_{\perp} . A similar situation applies to g_{\perp} . ^b The simulations were computed with the magnetic parameters of spin probe A, where $A_z = 35.8$, $A_x = 5.5$, $A_y = 5.7$, $g_z = 2.0022$, $g_x = 2.0084$, and $g_y = 2.0060$,^{24,25} in agreement with the experimental A_0 and A_{\parallel} values determined in this work.

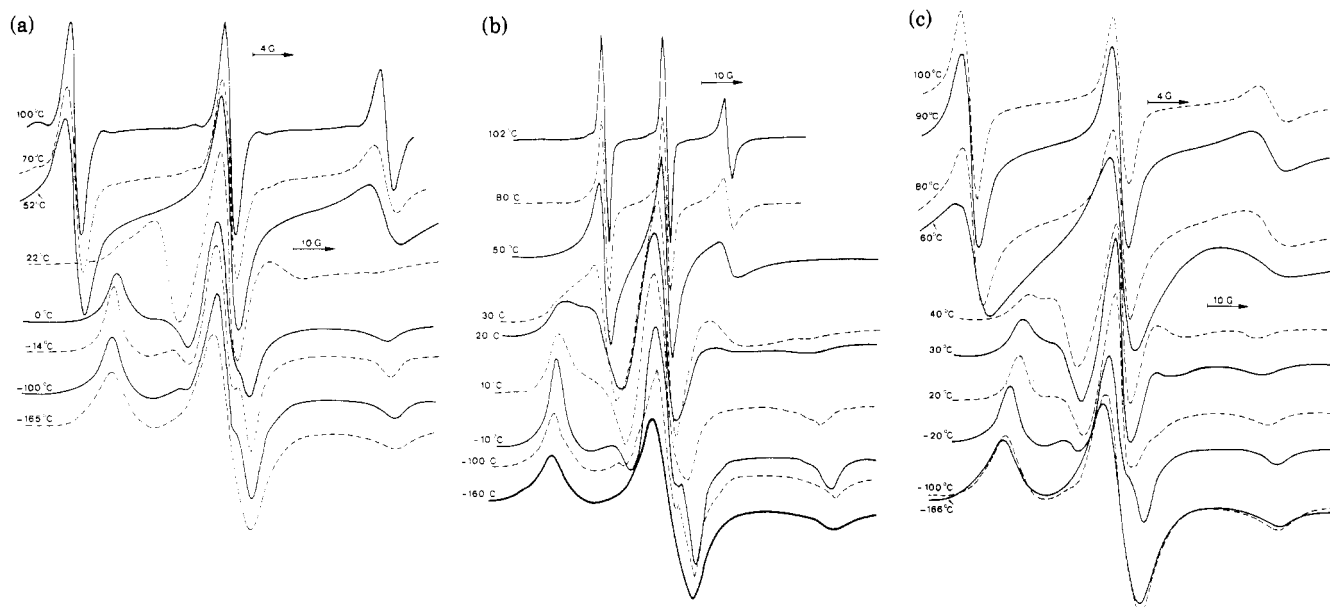


Figure 8. ESR spectra of the probes B (a), C (b), and D (c) in polyester TO29.

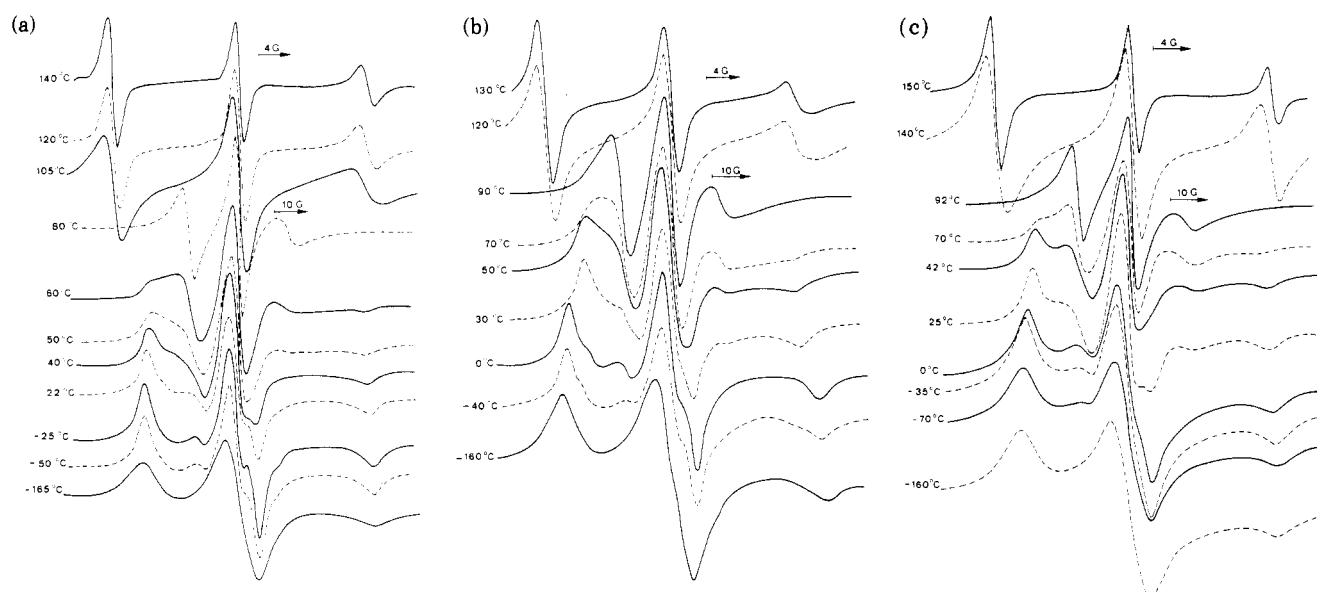


Figure 9. ESR spectra of the probes B (a), C (b), and D (c) in polyester TO11.

The a and b coefficients depend on the intrinsic line width and the rotational diffusion model adopted. From an analysis of the rigid-limit spectra of TO11 and TO29 it can be seen that the values of a and b given by Goldman et al.^{26a} for an intrinsic line width of 3 G have to be used for estimating τ_c .

Results

Representative ESR spectra of polyesters TO29 and TO11 are shown in Figures 8 and 9. Above the melting

point, i.e., 70 °C for TO29 and 125 °C for TO11, the hyperfine pattern is characteristic of rapidly tumbling nitroxides: the ESR spectrum consists of three sharp lines. In the ESR spectra of probes B and C dissolved in TO29, the low-field and the center-field lines have approximately equal heights (Figure 8a,b). On the contrary, the spectra of probe D registered above 95 °C show the unusual feature that the low-field line is more intense than the center-field line (Figure 8c), which can be explained only if the effects on the line shape of an anisotropic rotational diffusion of

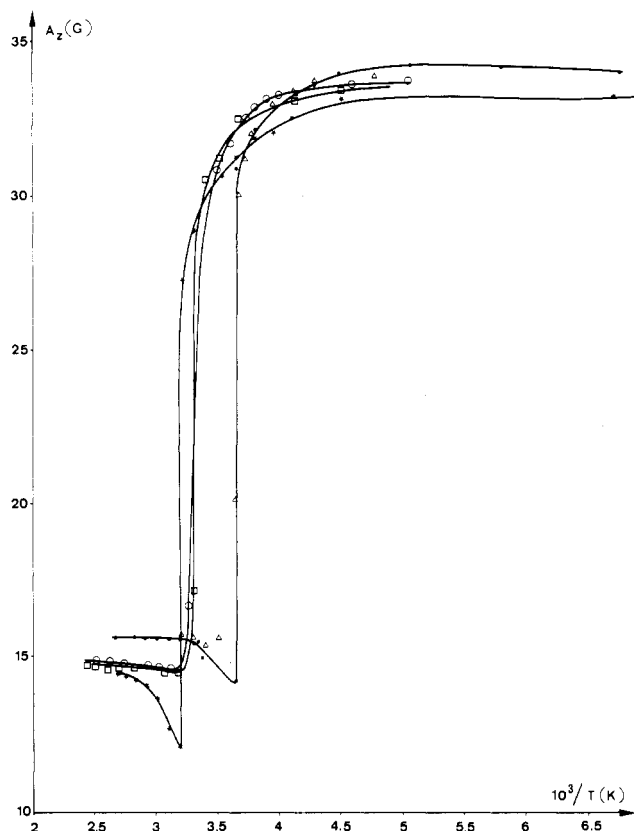


Figure 10. Plots of A_z vs. reciprocal temperature in the ESR spectra of (●) A-, (○) B-, (□) C-, and (★) D-doped polyester TO29 and (△) A-doped PEO.

the probes are taken into account.^{27,28} The same behavior is observed at high temperature for the probes dissolved in TO11.

Around the crystal \leftrightarrow mesophase transition, in all cases the experimental ratio

$$(R_+ + R_- - 2)/(R_+ - R_-)$$

approaches the theoretical value of $C/B = K$, which is indicative of radicals undergoing (at least temporarily) isotropic reorientation.

As the temperature is decreased, the low-field line becomes less intense than the center-field line and the spectra are markedly broadened and increasingly asymmetric. These features are characteristic of probes undergoing anisotropic reorientation.

At a temperature that depends on the polyester structure and the spin-probe nature, a subsequent overlapping of lines occurs, and a redistribution of the lines, characteristic of slowly tumbling nitroxides, is observed. The separation of the outer hyperfine extrema $2A_z'$ increases with decreasing temperature until it becomes experimentally indistinguishable from the rigid-limit value $2A_z$ (Figures 10 and 11). At the lowest temperature, the spectrum reflects the complete development of the anisotropic hyperfine interaction and the anisotropic g factor.

Such temperature changes in the ESR spectra can be attributed to changes in the rotational motion of the nitroxide radicals. As a first step, we have estimated the correlation times by assuming that the different probes undergo an isotropic reorientation over the whole temperature range. Such an assumption has been usually done by authors who have studied the dynamics of spin labels and probes in polymeric solids and melts.²⁹⁻³³ As pointed out by Smith²⁸ and Kovarskii et al.,³⁴ the value of τ_c calculated from the isotropic diffusion model accurately re-

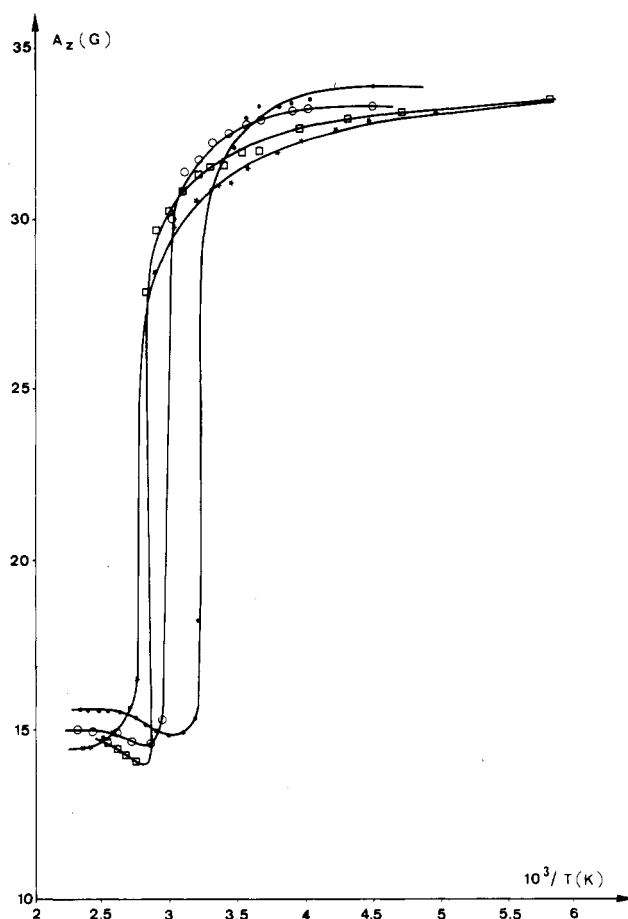


Figure 11. Plots of A_z vs. reciprocal temperature in the ESR spectra of (●) A-, (○) B-, (□) C-, and (★) D-doped polyester TO11.

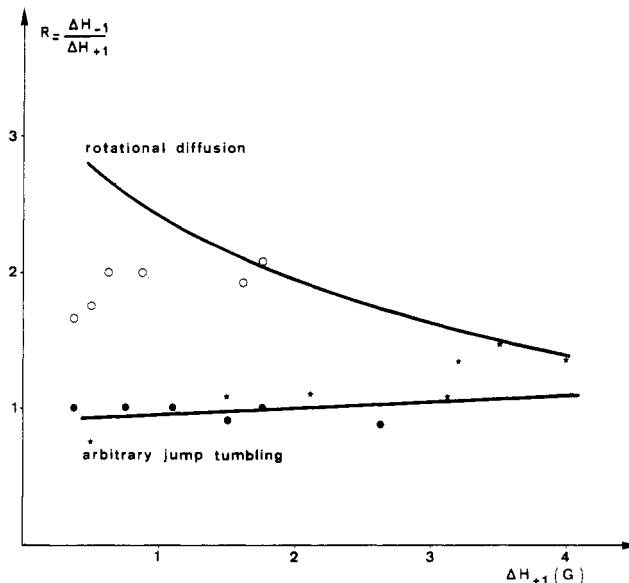


Figure 12. Dependence of the parameter R on ΔH_{+1} for polyester TO29: experimental values (●) for probe A, (○) for probe B, and (★) for probe D.

flects in order of magnitude the correlation time of rotational diffusion of the probe. Indeed, it is close to the average τ_c for anisotropic motion that Freed defines as $\tau_c = (6\bar{D})^{-1}$, with $\bar{D} = (D_{\parallel}D_{\perp})^{1/2}$. We will discuss this point later.

The slow-motional correlation times were calculated by using the parameter $S = A_z'/A_z$. We have first analyzed the rotational diffusion character using the parameter $R = \Delta H_{-1}/\Delta H_{+1}$, where ΔH_{-1} is the shift of the absorption

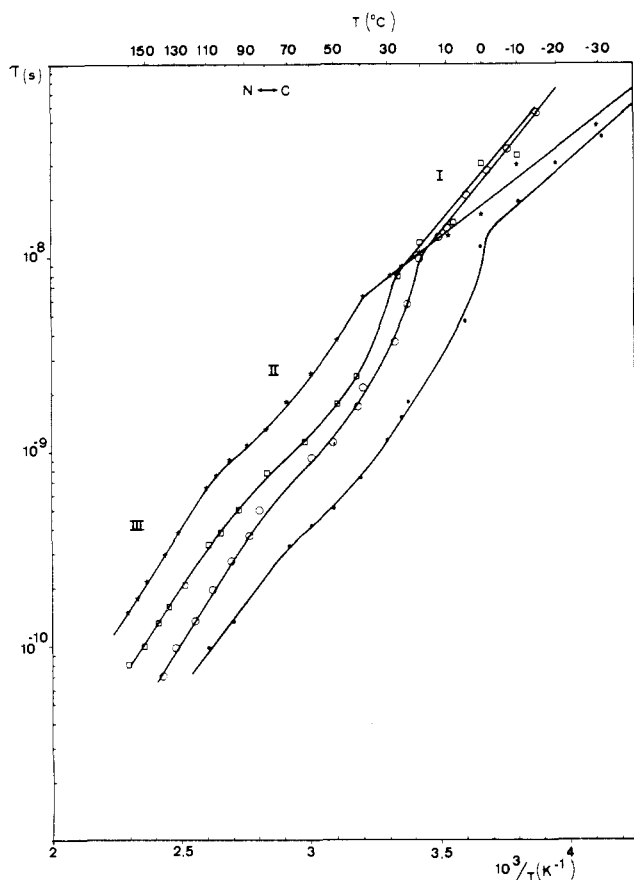


Figure 13. Rotational correlation times calculated from the spectra of polyester TO29 using the method of Waggoner et al.³⁶ and the approach of Goldman et al.^{26a} (●) probe A; (○) probe B; (□) probe C; (★) probe D.

extremum in the high field with respect to the rigid limit and ΔH_{+1} is the low-field shift. Figure 12 illustrates the theoretical dependences of the parameter R on ΔH_{+1} for Brownian rotational diffusion and arbitrary jump tumbling models. From Kuznetsov's studies³⁵ it appears that the nonsphericity of the radicals used causes only a small change in R : there is no correlation between the variation of R and the axial ratio of the probe. Only the character of the rotational motion (diffusional or jump tumbling) is adequate to account for the variation of R . For probes A and D, all the experimental R values are between 0.8 and 1.2 and closely correspond to the theoretical values for an arbitrary jump tumbling model. For the two pyrroline derivatives B and C, R lies in the range 1.8 and 2, approximately corresponding to the theoretical value of the Brownian rotational diffusion model. Thus, if the molecular size of the probe is sufficiently large, the model of continuous rotational diffusion is valid. By decreasing the size of the probe, the probability of jump tumbling increases. Note that for probe D, only the size of the ring seems to be of importance in the definition of the motion; the flexible aliphatic chain does not seem to intervene. The fast-motional correlation times were estimated from eq 4. It can be seen from Figures 13 and 14 that correlation times do not fit an expression of the Arrhenius type over the whole temperature range. Although we are studying the dynamics of the spin probe, it is clear that it is sensitive to the dynamics of the surrounding environment and that TO29 and TO11 display more than one relaxation process. The manner in which the spectrum shape, the extrema separation, and correlation times vary with temperature shows that there are only three regions of different mobility to be considered for TO29 in the temperature range -30

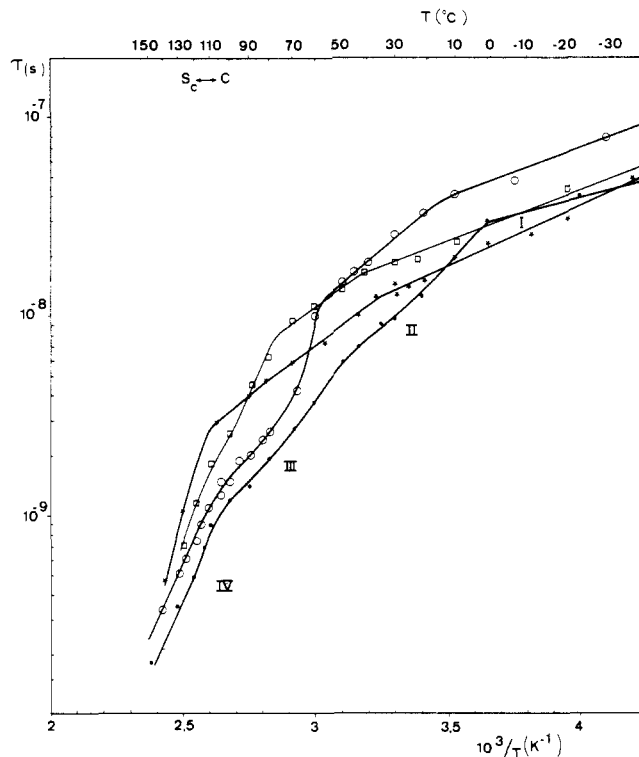


Figure 14. Rotational correlation times calculated from the spectra of polyester TO11 using the method of Waggoner et al.³⁶ and the approach of Goldman et al.^{26a} (●) probe A; (○) probe B; (□) probe C; (★) probe D.

Table II
Transition Temperatures Determined from the $\log \tau_c$ vs. $1/T$ Dependences for Probes A, B, C, and D Mixed with Either Polyester TO29 or TO11

spin probe	transition temperature, °C	
	polyester TO29	polyester TO11
A	0, ^a 70 ^b	0, 45, ^a 105 ^b
B	20, ^a 75 ^b	10, 60, ^a 105 ^b
C	30, ^a 80 ^b	40, 77, ^a 105 ^b
D	40, ^a 100 ^b	35, 85, ^a 110 ^b

^a These temperatures closely correspond to T_{50G} and, hence, are related to T_g . ^b These temperatures are in agreement with the crystal \leftrightarrow mesophase transition.

to +150 °C. Spectra obtained for spin probes added to TO11 are indicative of four relaxation processes. The transition temperatures are given in Table II.

As mentioned above, these values for correlation times are only approximate because both the analysis based on Freed and co-workers' S parameter formalism and eq 4 assume isotropic rotational reorientation. In fact, for the polyesters under investigation, the ratio C/B approaches the theoretical value K only around the melting point, i.e., 70–80 °C for TO29 and 105–125 °C for TO11. At lower temperatures experimental data are indicative of radicals undergoing anisotropic reorientation. For probe A, such an anisotropic rotation is surprising in view of its small size and near-spherical shape (in comparison with probe C or D). As will be shown later, the medium in which it is rotating must show sufficient ordering and/or high viscosity to restrict totally isotropic rotation.

The role of anisotropic rotation has not yet aroused much attention in ESR studies of condensed polymeric systems although one observes in some published spectra of polymers with high T_g a splitting of the high-field peak into two components, which may reflect an anisotropic rotation. In fact, such complex spectra have been usually

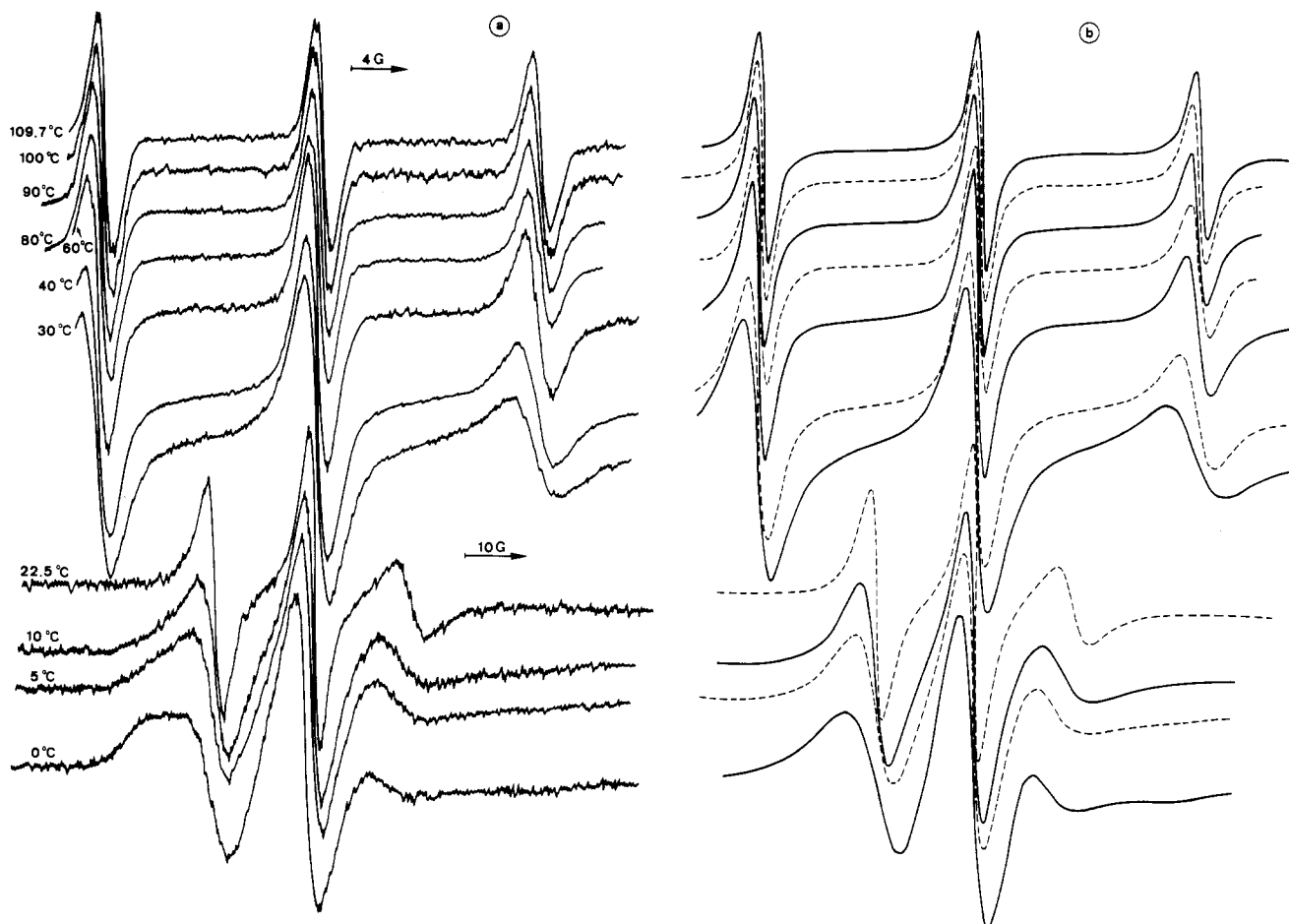


Figure 15. Experimental (a) and simulated (b) spectra of probe A doped polyester TO29.

interpreted by considering that some radicals experience a different rate of tumbling than others in the polymeric environment and have been resolved into a solid-state component and a mobile component.³⁷⁻⁴¹ Such an analysis seems reasonable in the case of dimethylsiloxane (DMS)/bisphenol A carbonate (BPAC) block copolymers, for which there is evidence that the BPAC blocks associate into rigid domains that act as physical cross-links for the more mobile DMS blocks. These copolymers show a two-phase behavior in that the mechanical properties exhibit two major relaxations, which have been attributed to two glass transition temperatures. Using the methods of pulsed and CW electron paramagnetic resonance, Brown⁴¹ has shown that in the temperature range 220–380 K the observed spectra are a superposition of a fast-phase spectrum ($\tau_c < 10^{-9}$ s) and a slow-phase spectrum ($\tau_c > 10^{-7}$ s). The fast phase corresponds to spin probes located in rubbery DMS block environments and the slow phase is identified with spin probes located in domains of associated BPAC blocks. However, Bullock et al.³² have shown that the polymer segment motions involved in the low-temperature relaxation processes may give rise to split spectra because of the anisotropic reorientation of the radicals. Moreover, Mason et al.⁴² have given an analysis for motional effects on ESR spectra of spin labels undergoing very anisotropic rotational relaxation in isotropic liquids. This analysis examines the spectral consequences for cases where the nitroxide is undergoing rapid rotation about a single bond, while the macromolecule to which it is attached is reorienting slowly. This approach was found to be in good agreement with experiments of Wee and Miller⁴³ on spin-labeled poly(benzyl glutamate) in dimethylformamide. For the polyesters under investigation,

the occurrence of a liquid crystalline phase evidently favors an anisotropic rotation of the nitroxide probes. In order to quantify the effects of an anisotropic rotation, experimental spectra of probe A in TO29 and TO11 were analyzed by comparing them with simulated line shapes. In calculations of the simulated spectra we used the program published by Freed.¹⁹ The values of the g tensor and nitrogen hyperfine tensor used in the calculation are given in Table I.

The magnetic x axis is taken as being along the N–O bond, the z axis along the $2p\pi$ orbital of the nitrogen, and the y axis perpendicular to the other two. The principal axes of the diffusion tensor \mathbf{R} are labeled x' , y' , and z' . As well as for PD-tempon, agreement between calculated and experimental spectra is obtained for $z' = y$. In this way, it was possible to simulate quite satisfactorily the spectra of probe A in polyester TO29 (Figure 15) and TO11 (Figure 16). However, in the slow-motional region, certain computational limitations involved in the calculation of the simulated spectra hindered us from calculating line shapes for $\tau > 7 \times 10^{-9}$ s.

Discussion

$T < \text{Melting Point}$. At a critical temperature that depends on the probe size and the polyester structure, the plot of the extrema separation in the ESR spectra vs. the reciprocal temperature (Figures 10 and 11) shows a sharp decrease, indicating the onset of rapid motion of the spin probe which averages the anisotropic components to produce spectra characteristic of rapid nitroxide rotation, i.e., spectra presenting no more complex structure and varying only in line width. From a study of the temperature-dependent ESR spectra of a series of nitroxide-doped poly-

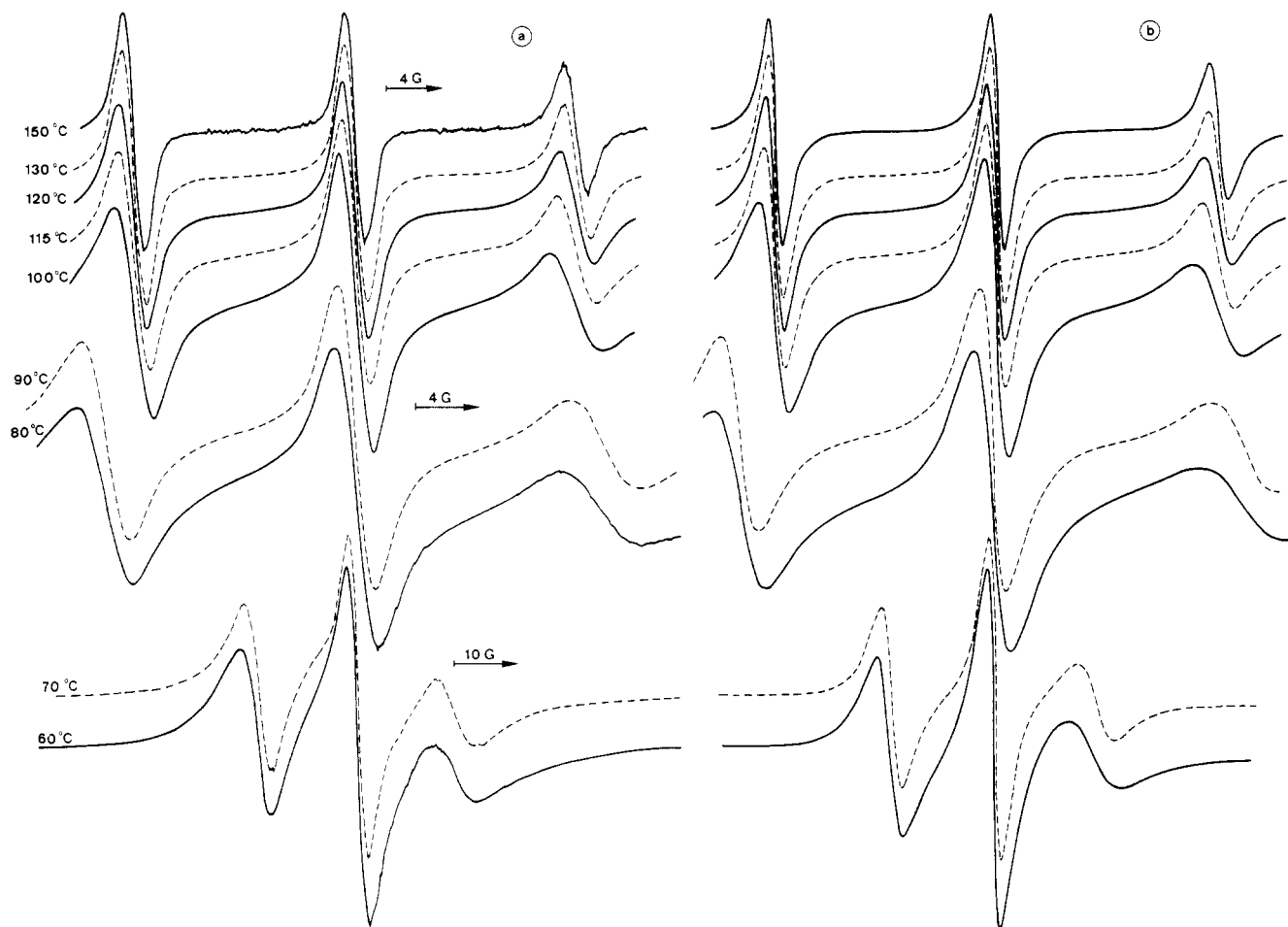


Figure 16. Experimental (a) and simulated (b) spectra of probe A doped polyester TO11.

mers and copolymers, an empirical parameter $T_{50\text{G}}$ was selected.⁶ This parameter was defined as the temperature at which the peak-to-peak separation of the two extrema of the three-line nitroxide spectrum was equal to 50 G. Several authors have demonstrated that $T_{50\text{G}}$ correlates with T_g if the probe is sufficiently large. As shown in Figure 17, $T_{50\text{G}}$ is highly dependent on the spin probe molecular weight but tends to approach a limiting value of 36 and 81 °C for TO29 and TO11, respectively.

Polyester TO29. It can be seen from Figure 10 that the temperature region -3 to $+2$ °C at which the outermost separation of the ESR spectrum changes most drastically is the same whether spin probe A is mixed with polyester TO29 or poly(ethylene oxide) (PEO). In the latter case, $T_{50\text{G}}$ has been previously assigned to the onset of the β -relaxation process,^{31b,33} which is due to the diffusional segmental motion in the amorphous region. Because of the relatively high frequency of the ESR measurements, the β process of PEO appears at a temperature considerably above that determined by DSC (literature values range from -115 to -40 °C).^{31b} On the other hand, it can be seen from Figure 13 that within the temperature range $T_{50\text{G}}$ to 80 °C, the $\log \tau$ vs. $1/T$ dependences for polyester TO29 are almost linear. The activation energies of rotational reorientation of the spin probes determined from these dependences lie in the range 7.5–9.5 kcal/mol. A virtually identical value of the activation energy also follows for the β process of PEO from the ESR results obtained by Lang et al.³³ assuming an isotropic rotational reorientation of the nitroxide radical. As reported by several authors,^{30,32,33,44} the ESR measurements give for the β -relaxation process activation energies that usually appear lower than those found by other techniques. These dif-

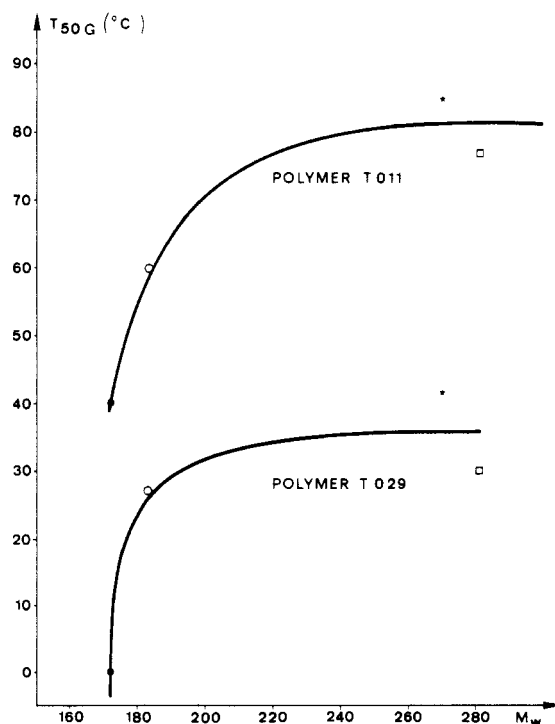


Figure 17. Dependence of $T_{50\text{G}}$ on the probe molecular weight.

ferences may be explained by the high-temperature dependence of the activation energy for the β -relaxation process: as the temperature or the frequency of the test increases, the "apparent" activation energy decreases. Hence, experimental data suggest that the relaxation

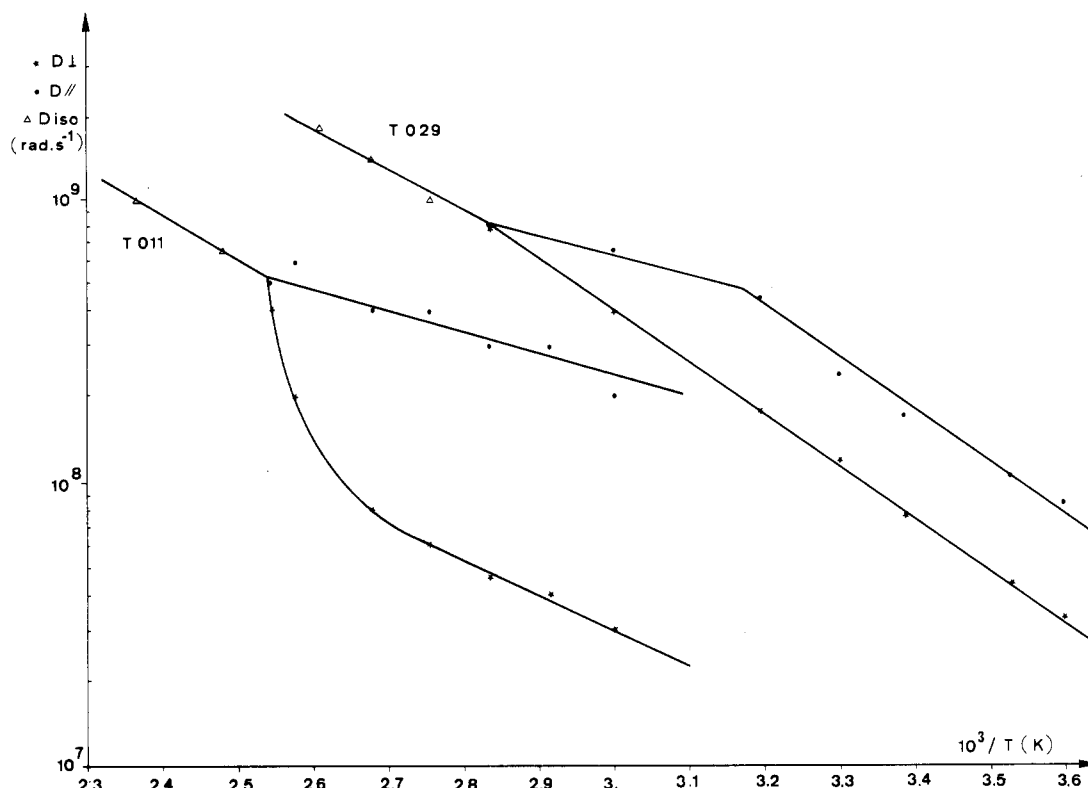


Figure 18. Rotational diffusion constants D_{\parallel} and D_{\perp} calculated for probe A mixed with either polyester TO29 or TO11.

process, which is reflected at T_{50G} by the different spin probes mixed with polyester TO29, is due to the diffusional segmental motion of the flexible "ether" sequences located in the amorphous isotropic regions. From a conformational energy point of view, one would expect only the central $-\text{CH}_2\text{CH}_2\text{O}-$ units, which are relatively free from restraints caused by the presence of the rigid mesogenic groups, to be involved in the diffusional segmental motion. Taking into account the time-temperature superposition principle, this relaxation process corresponds to T_{gu} , the lower of the two glass transitions evidenced by DSC. The lack of discontinuity in the $\log \tau$ vs. $1/T$ dependences (Figure 13) from -3 to $+2$ °C up to 70 – 80 °C suggests that the radicals mixed with polyester TO29 are located predominantly in the amorphous isotropic regions and do not respond to T_{gu} .

Polyester TO11. Similar arguments based on the manner in which the ESR spectrum shape (Figure 9), the extrema separation (Figure 17), and correlation times (Figure 14) vary with temperature lead to the conclusion that at T_{50G} , the rotational mobility of spin probes mixed with polyester TO11 also reflects the β -relaxation process. However, it is related to the marked increase in heat capacity that is observed by DSC between 20 and 50 °C, that is to say T_{gu} .

From the data presented in Figures 2 and 14, it can be seen that there is another relaxation process at lower temperatures: a small increase in heat capacity extends from -40 to 10 °C and a slight increase in the nitroxide radical mobility occurs at a temperature that depends on the probe size but is in the range 0 – 40 °C (Table II). It is noteworthy that DSC and ESR measurements have given the same temperatures for the T_{gu} transition of polyester TO29. Thus, it is tempting to associate the lower transition of polyester TO11 with a low content of an isolated disordered structure. It would be of obvious value to have ESR spin probe data of a series of samples submitted to different heat treatments.

Computer simulations of the ESR spectra are of considerable help in quantifying the effects of an anisotropic

rotational reorientation of the spin probe. The diffusion parameter $N = D_{\parallel}/D_{\perp}$, where D_{\parallel} and D_{\perp} are the components of the rotational diffusion about z' and about x' , respectively, is 1 for isotropic rotational motion and becomes larger as anisotropy of motion increases. One would expect a small N value for probe A in view of its near-spherical shape. For example, theoretically N equals 1.35 for 2,2,6,6-tetramethylpiperidonyl-1-oxy (Tempone),²⁴ the size and shape of which are very similar to those of Tempol. In the present experiments, however, N is larger. It can be seen from Figure 18 that, at low temperatures, N lies in the range 2–2.5 for probe A mixed with polyester TO29, which indicates a slightly higher asymmetry in the rotational diffusion. This result may be explained by an interaction of nitroxide with the surrounding polymer. If probe A is hydrogen bonded to polyesters as observed, for example, by Veksli and Miller⁴⁵ in the case of poly(methyl methacrylate), it may lead to anisotropic motion. By assuming that the probe undergoes an isotropic reorientation, Veksli and Miller have calculated a rotational correlation time of 2.2×10^{-9} s for the fast-motional component in the PMMA–probe A system at 100 °C. By contrast, tempone doped in PMMA, a case in which the spin probe cannot be hydrogen bonded to PMMA, has a correlation time of 3×10^{-11} at the same temperature. From Figure 13 it can be seen that we do not observe such a large difference in the correlation time between probes A and B, which may hydrogen bond with polyester TO29, and non-hydrogen-bonding probes C and D. Taking into account the molecular size of the probes, the difference in correlation time is similar to that observed with non-hydrogen-bonding polymers.⁶ Besides, at about 70 – 80 °C, the representative ESR spectra in Figure 15, the value of the experimental ratio $C/B = R_+ + R_- / R_+ - R_-$, and the data obtained by careful simulation are indicative of radicals undergoing isotropic reorientation, which should be due to probes no longer remaining hydrogen bonded. Inasmuch as the chemical structure of polyesters TO11 and TO29 are virtually identical, except that TO29 contains longer flexible

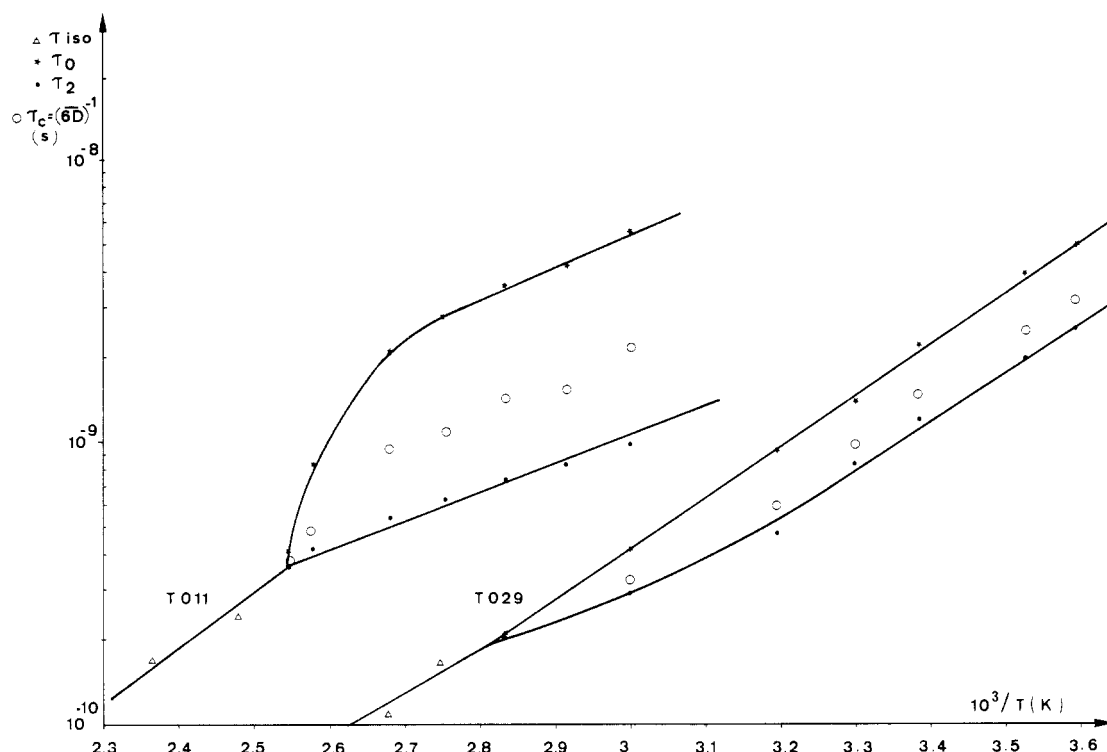


Figure 19. Correlation times determined from simulated spectra for probe A mixed with either polyester TO29 or TO11.

spacers, it seems surprising that at the same temperature, the rotational diffusion constant D_{\parallel} of probe A mixed with polyester TO11 is approximately 7 times D_{\perp} (Figure 18). More probably, the medium in which probe A is rotating below 70–80 °C may show sufficient ordering to restrict isotropic rotation. The value of 7, obtained for the diffusion parameter N for probe A mixed with polyester TO11, reflects the much higher degree of order in this polyester.

The correlation times determined by employing the simulation procedure are given in Figure 19. As follows from Figures 13, 14, and 19, correlation times calculated from the isotropic diffusion model are in good agreement with the average τ_c for anisotropic motion at high temperature but they become slightly larger in the slow-motional region.

Crystal \leftrightarrow Mesophase Transition. It is clear that the crystal \leftrightarrow liquid crystal transition, which occurs at 70–80 and 105–125 °C for polyesters TO11 and TO29, respectively, causes a real modification of the environment of the probe:

First, it can be seen from Figures 18 and 19 that, approximately 20 °C below the crystal \leftrightarrow mesophase transition, a “premelting” effect occurs. The observed values for N become smaller as the temperature increases. This result means that there is a decrease in the degree of anisotropy with increasing temperature. At the crystal \leftrightarrow mesophase transition, N equals 1, which indicates that the rotation of probes is temporarily isotropic. A further increase in temperature results in a marked change of the ESR spectrum shape: the relative intensities of the low-field and the center-field lines progressively change. For example, it can be seen from Figure 9 that the spectra of doped polyester TO11 recorded above 130 °C show the unusual feature that the low-field line is sharper than the center-field line. Such a behavior has already been observed^{27,28} and can be readily explained if the effects on the line shape of the anisotropic rotational diffusion of the spin probes are taken into account. It suggests that the orientation of the anisotropic diffusion axis with respect

to the nitroxide radical axis changes upon passing through the crystal \leftrightarrow liquid crystal transition.

Secondly, at 70–80 and 105–125 °C for polyesters TO11 and TO29, respectively, there is a break in the Arrhenius plot that corresponds to an increase in the spin-probe mobility (Figures 13 and 14). This may be due to a dynamic process of the phenyl rings. Indeed, earlier proton-decoupled ^{13}C solid-state NMR studies of polyester TO11² have shown that at the crystal \leftrightarrow liquid crystal transition, the width of the aromatic carbons line strongly decreases and the line shape is modified. By comparing experimental spectra with simulated line shapes, the motional process of the phenyl rings above the crystal \leftrightarrow liquid crystal transition has been associated with a rotation about the $\text{C}_1\text{--C}_4$ axis. It should be noted that such a motion does not alter the mean orientation of the mesogenic groups.

Acknowledgment. We are obliged to Dr. B. Fayolle for kindly placing at our disposal the polyesters. We are also obliged to Dr. C. Taupin for very fruitful discussions regarding the results of this work.

References and Notes

- (1) (a) A. Roviello and A. Sirigu, *J. Polym. Sci., Polym. Lett. Ed.*, **13**, 455 (1975); *Makromol. Chem.*, **180**, 2543 (1979); (b) A. C. Griffin and S. J. Havens, *J. Polym. Sci., Polym. Phys. Ed.*, **19**, 951 (1981); *Mol. Cryst. Liq. Cryst., Lett.*, **49**, 239 (1979); (c) S. Antoun, R. W. Lenz, and J. I. Jin, *J. Polym. Sci., Polym. Chem. Ed.*, **19**, 1901 (1981); (d) L. Strzelecki and D. van Luyen, *Eur. Polym. J.*, **16**, 299, 303 (1980); (e) A. Blumstein and S. Vilasagar, *Mol. Cryst. Liq. Cryst., Lett.*, **56**, 263 (1979); (f) A. Blumstein, K. N. Sivarama Krishnan, S. B. Clough, and R. B. Blumstein, *ibid.*, **49**, 255 (1979); (g) P. Meurisse, C. Noël, L. Monnerie, and B. Fayolle, *Br. Polym. J.*, **13**, 55 (1981).
- (2) P. Sergot, F. Lauprêtre, C. Louis, and J. Virlet, *Polymer*, **22**, 1150 (1981).
- (3) H. Kresse, 12th Europhysics Conference on Macromolecular Physics, “Molecular Mobility in Polymer Systems”, Leipzig, 1981, p 219.
- (4) G. Kothe, K. H. Wassmer, E. Ohmes, M. Portugall, and H. Ringsdorf, in “Liquid Crystals of One- and Two-dimensional Order”, W. Helfrich and G. H. Eppke, Eds., Springer-Verlag, Berlin, 1980, Vol. 11, p 259.

- (5) H. Kresse and R. V. Talrose, *Makromol. Chem., Rapid Commun.*, **2**, 369 (1981).
- (6) P. Törmälä, *J. Macromol. Sci., Rev. Macromol. Chem.*, **C17**, 298 (1979).
- (7) L. Bosio, B. Fayolle, C. Friedrich, F. Lauprêtre, P. Meurisse, C. Noël, and J. Virlet, in "Liquid Crystals and Ordered Fluids", A. Griffin and J. Johnson, Eds., Plenum Press, Vol. 4 (in press).
- (8) B. Fayolle, C. Noël, and J. Billard, *J. Phys. (Paris)*, **40**, C3-485 (1979).
- (9) E. G. Rozantsev and V. D. Sholle, *Synthesis*, **4**, 190 (1971).
- (10) R. Briere, H. Lemaire, and A. Rassat, *Bull. Soc. Chim. Fr.*, **11**, 3273 (1965).
- (11) J. C. Williams, R. Mehlhorn, and A. D. Keith, *Chem. Phys. Lipids*, **7**, 207 (1971).
- (12) H. Kelker, and R. Hatz, "Handbook of Liquid Crystals", Verlag Chemie, 1980.
- (13) C. Noël, L. Monnerie, M. F. Achard, F. Hardouin, G. Sigaud, and H. Gasparoux, *Polymer*, **22**, 578 (1981).
- (14) L. Liebert, L. Strzelecki, D. Van Luyen, and A. M. Levelut, *Eur. Polym. J.*, **17**, 71 (1981).
- (15) F. Volino, A. F. Martins, R. B. Blumstein, and A. Blumstein, *C. R. Hebd. Seances Acad. Sci.*, **292**, 829 (1981); *J. Phys. (Paris)*, *Lett.* **42**, L305 (1981).
- (16) S. Maret, A. Blumstein, and S. Vilasagar, *Polym. Prepr., Am. Chem. Soc., Div. Polym. Chem.*, **22**, 246 (1981).
- (17) F. Hardouin, M. F. Achard, H. Gasparoux, L. Liebert, and L. Strzelecki, *J. Polym. Sci., Polym. Phys. Ed.*, **20**, 975 (1982).
- (18) J. H. Freed, G. V. Bruno, and C. F. Polnaszek, *J. Phys. Chem.*, **75**, 3385 (1971).
- (19) J. H. Freed, in "Spin Labeling: Theory and Applications", L. J. Berliner, Ed., Academic Press, New York, 1976, p 53.
- (20) J. H. Freed and G. K. Fraenkel, *J. Chem. Phys.*, **39**, 326 (1963).
- (21) J. H. Freed, *J. Chem. Phys.*, **41**, 2077 (1964).
- (22) A. Hudson and G. R. Luckhurst, *Chem. Rev.*, **69**, 191 (1969).
- (23) P. L. Nordio, in "Spin Labeling: Theory and Applications", L. J. Berliner, Ed., Academic Press, New York, 1976, p 5.
- (24) J. S. Hwang, R. P. Mason, L. P. Hwang, and J. H. Freed, *J. Phys. Chem.*, **79**, 489 (1975).
- (25) S. Gade, A. Chow, and R. Knispel, *J. Magn. Reson.*, **40**, 273 (1980).
- (26) (a) S. A. Goldman, G. V. Bruno, and J. H. Freed, *J. Phys. Chem.*, **76**, 1858 (1972); (b) R. C. McCalley, E. J. Shimshick, and H. M. McConnell, *Chem. Phys. Lett.*, **13**, 115 (1972).
- (27) P. L. Nordio, *Chem. Phys. Lett.*, **6**, 250 (1970).
- (28) P. M. Smith, *Eur. Polym. J.*, **15**, 147 (1979).
- (29) A. L. Kovarskii, J. Pláček, and F. Szöcs, *Polymer*, **19**, 1137 (1978).
- (30) A. M. Wasserman, T. A. Alexandrova, and A. L. Buchachenko, *Eur. Polym. J.*, **12**, 691 (1976).
- (31) (a) P. M. Smith, R. F. Boyer, and P. L. Kumler, *Macromolecules*, **12**, 61 (1979); (b) R. F. Boyer and P. L. Kumler, *ibid.*, **10**, 461 (1977); **9**, 903 (1976).
- (32) A. T. Bullock, G. G. Cameron, and P. M. Smith, (a) *J. Polym. Sci., Polym. Phys. Ed.*, **11**, 1263 (1973); (b) *Eur. Polym. J.*, **11**, 617 (1975).
- (33) M. C. Lang, C. Noël, and A. P. Legrand, *J. Polym. Sci., Polym. Phys. Ed.*, **15**, 1329 (1977).
- (34) A. L. Kovarskii, A. M. Vasserman, and A. L. Buchachenko, *Vysokomol. Soedin., Ser. A*, **13**, 1647 (1971).
- (35) A. N. Kuznetsov and B. Ebert, *Chem. Phys. Lett.*, **25**, 342 (1974).
- (36) A. S. Waggoner, O. H. Griffith, and C. R. Christensen, *Proc. Natl. Acad. Sci. U.S.A.*, **57**, 1198 (1967).
- (37) S. Vivatpanachart, H. Nomura, and Y. Miyahara, *Polym. J.*, **13**, 481 (1981).
- (38) S. C. Gross, *J. Polym. Sci., Part A-1*, **9**, 3327 (1971).
- (39) G. P. Rabold, *J. Polym. Sci., Part A-1*, **7**, 1203 (1969).
- (40) R. F. Boyer and P. L. Kumler, 10th Europhysics Conference on Macromolecular Physics: "Structure and Motion in Polymeric Glasses", Noordwijkerhout, 1980, p 190.
- (41) S. Lee and I. M. Brown, *Macromolecules*, **12**, 1235 (1979). I. M. Brown, *Macromolecules*, **14**, 801 (1981).
- (42) R. P. Mason, C. F. Polnaszek, and J. H. Freed, *J. Phys. Chem.*, **78**, 1324 (1974).
- (43) E. L. Wee and W. Miller, *J. Phys. Chem.*, **77**, 182 (1973).
- (44) P. Törmälä, *Eur. Polym. J.*, **10**, 519 (1974).
- (45) Z. Veksli and W. G. Miller, *Macromolecules*, **10**, 1245 (1977).

Small-Angle Neutron Scattering and Light Spectroscopy Investigation of Polystyrene Gels under Osmotic Deswelling

Jacques Bastide,* Robert Duplessix, and Claude Picot

Centre de Recherches sur les Macromolécules, 67083 Strasbourg Cedex, France

Sauveur Candau

Laboratoire d'Acoustique Moléculaire, Université Louis Pasteur, 67070 Strasbourg Cedex, France. Received November 29, 1982

ABSTRACT: Neutron scattering experiments on a partially labeled gel and quasi-elastic light scattering measurements are reported. The radius of gyration of the elementary mesh of the labeled network is shown to remain nearly constant when the gel is deswollen by a factor of 4 in volume. This result is in contradiction with the fundamental hypothesis of the classical theories of gel swelling; however, it can be understood by considering a rearrangement of the network at a scale larger than the mesh. The cooperative diffusion constant D_c of the osmotically deswollen gels was measured by using the quasi-elastic light scattering. The apparent scaling law of D_c vs. ϕ , the polymer volume fraction of the gel, is shown to differ significantly from that corresponding to a series of gels swollen at equilibrium in a pure solvent. This result is interpreted in the framework of a phenomenological scaling approach, consistent with the neutron scattering results. This approach allows the calculation of the variation with ϕ of K_{os} and G , the osmotic bulk modulus and the shear modulus of the gel, respectively, which appear in the expression for D_c .

Introduction

In order to understand the thermodynamic behavior of polymeric networks, a knowledge of the relation between macroscopic and microscopic properties is required. Most of the available theories of polymer networks are based on some fundamental assumptions regarding the local deformation of polymer chains as a function of the network state of strain or swelling. However, for a long time the

validity of these assumptions could not be directly checked. In this regard, important progress has been achieved recently through experiments with small-angle neutron scattering (SANS). SANS associated with partial deuteration is a very efficient technique for characterizing the conformation of the elastic chains in a cross-linked polymer. The angular dependence of the neutron scattering intensity given by networks containing small amounts of